Electronic Supplementary Information:

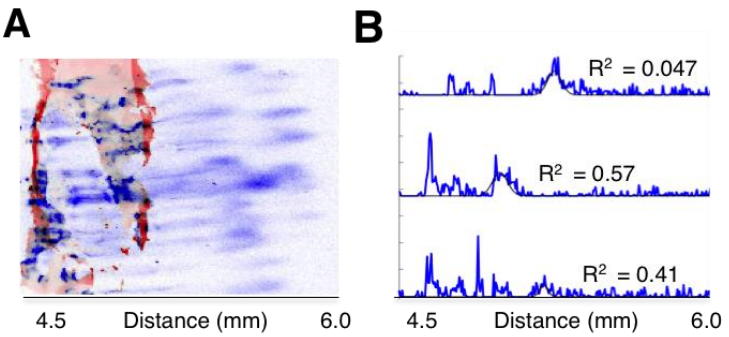

Denaturing Lysis Buffer[1]	Higher detergent IEF lysis buffer
7 M Urea	7 M Urea
2 M thiourea	2 M thiourea
4% w/v CHAPS	5% w/v CHAPS
1% v/v Triton-X 100	2.5 % v/v Triton-X 100

Figure S1. *In situ* IEF of cells (9000 cells/cm^2 seeding density) using the previously reported[1] denaturing lysis buffer demonstrates limited solubilisation. (A) False-colour, inverted fluorescence micrographs of lamin A/C resulting from *in situ* IEF using the previously reported denaturing lysis buffer. (B) Example fluorescence intensity profiles of probed lamin A/C indicate poor Gaussian fit and un-analysable data. (C) Table of reformulation of the lysis buffer to include a higher concentration of detergents CHAPS and Triton-X 100. This reformulation was used for all data presented in the main text.

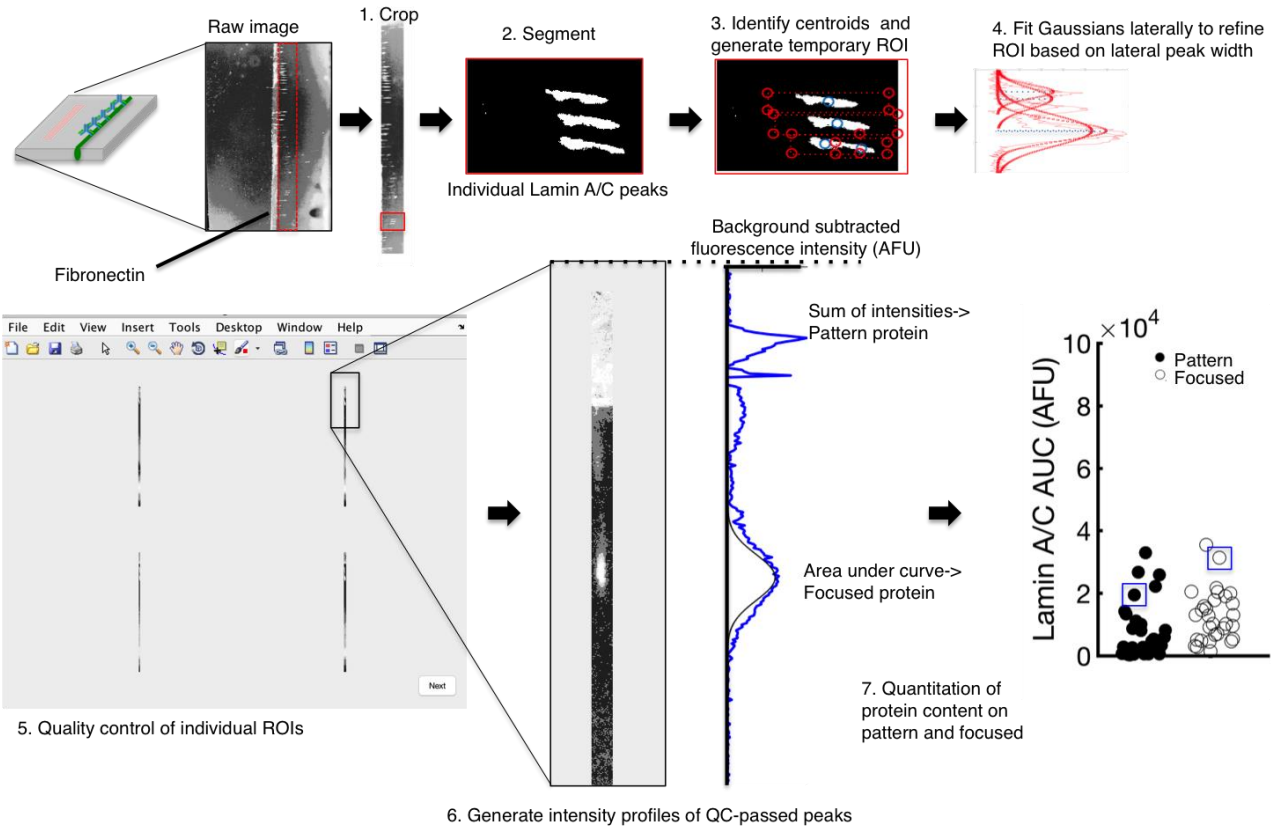

Figure S2. Workflow for image segmentation using a MATLAB GUI. The raw fluorescence image is first cropped based on user-based inputs on the bounds of the extracellular matrix protein pattern and end of separation lane. In the second step, the peaks are segmented via thresholding, converting to binary, and identifying centroids of each object (peak). Based on locations of the centroids, a temporary ROI is generated based on the values of the major and minor axis of the ellipse fitted to the identified peaks. Next, in step four, a Gaussian is fit *laterally* across each ROI from the cropped original (non-binary) image to identify the peak mean and width. From there, a new ROI is generated, which encompasses the entire peak (mean ± 4σ). A quality control (QC) step is performed in Step 5 by the user to remove overlapping peaks or other artefacts caused by dust, debris, etc. Following QC, background-subtracted intensity profiles are extracted from each ROI. The background is subtracted on a per-pixel basis. For quantitation, the sum of the intensities of the background-subtracted profile (ID) are obtained for the pattern protein content, and the area-under-the-curve (AUC) of the Gaussian fit to the focused peak for the focused protein content.

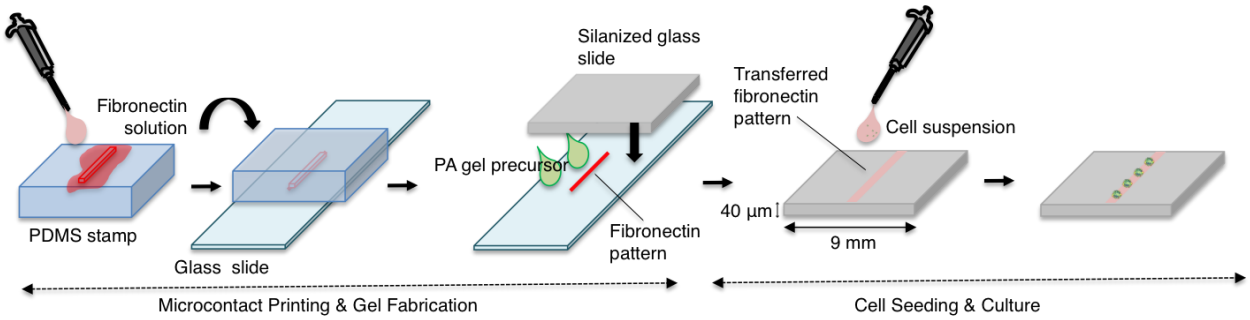

Figure S3. Schematic of microcontact printing of fibronectin-patterned substrate gels. The protocol for creating the substrates is described in the Materials and Methods section. Fibronectin solution is pipetted onto a PDMS stamp and inverted onto a standard microscope slide. Polyacrylamide gel is then polymerised between the patterned slide and a silanized glass slide. The fibronectin pattern transfers to the polyacrylamide gel. After, cells are seeded on top of the fibronectin-patterned substrate gel, and non-adhered cells, i.e., in the unpatterned regions, are washed away.

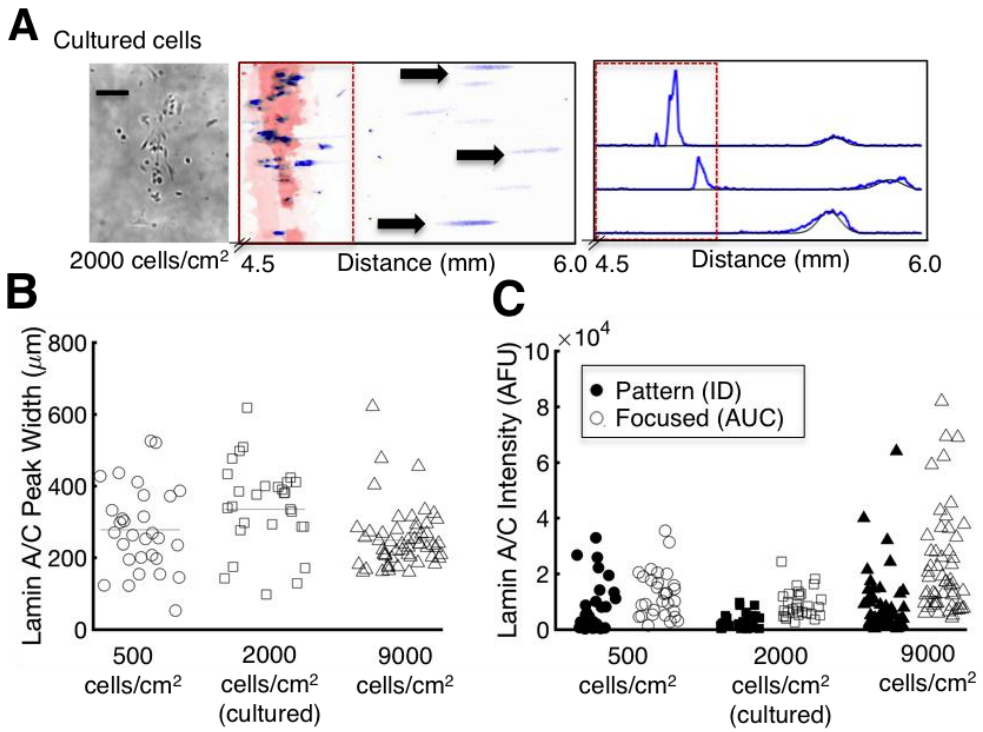

Figure S4. *In situ* IEF of cells seeded at a density of 500 cells/cm^2 and cultured for 4 days, for a final density of ~2000 cells/cm^2. (A) Brightfield images of cultured cells (left), and false-colour, inverted, fluorescence micrographs of lamin A/C that is retained on the fibronectin pattern and focused into a Gaussian peak (middle) and Gaussian fit of intensity profiles (right). (B) Separation performance, as measured by lamin A/C peak width, does not significantly change with culture duration. (C) Protein mass measurements of lamin A/C that is retained on the fibronectin pattern (ID) and focused (AUC). The data from the 500 and 9000 cells/cm^2 are the same as in the main text and are presented here for comparison purposes. Bars represent the mean. Scalebars, 200 μm. AFU, Arbitrary fluorescence units. ID, Integrated density. AUC, Area under curve. pI, isoelectric point.

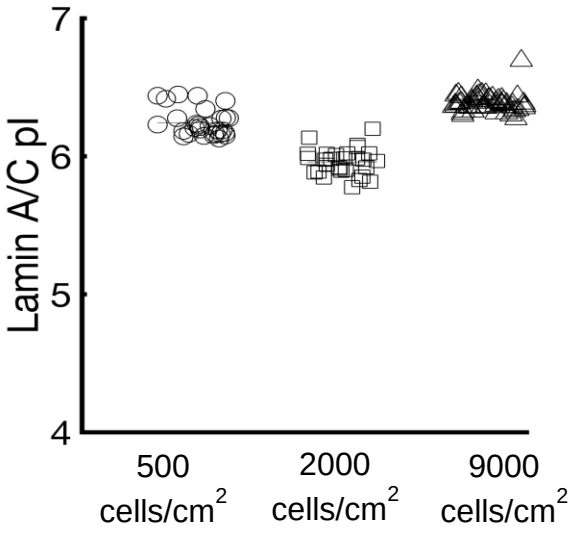

Figure S5. Measurement of lamin A/C pI. The pI was estimated for lamin A/C by using the peak location. The measured pI was 6.4 ± 0.06 (mean ± s.d., n = 112 peaks). Across devices and densities, the estimated pI of lamin A/C ranged from 6.0-6.4, which is close to those reported previously[1] and the predicted pI of 6.51 from proteomics software ExPASy.

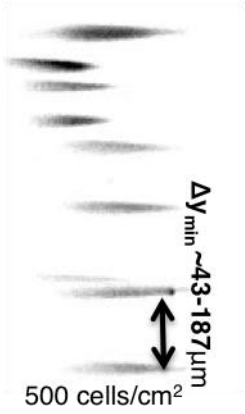

Figure S6. Lamin A/C peaks are resolved laterally at a low (500 cells/cm^2) cell density. To pattern single cells that were resolved laterally (perpendicular to the IEF axis), we used the characteristic diffusion equation ($\tau \sim X^2/D$) to determine the cell-to-cell spacing for minimally resolved lamin A/C peaks. We used already reported lamin A/C diffusion coefficients,[2] and factored in in-gel diffusivity of proteins in a 6%T, 3.3%C gel.[3] Given our 390 s assay time, we estimated cells needed to be spaced 43-187 µm (depending on which diffusivity used) apart. For the 500 cells/cm^2 seeding density, the peaks were spaced 74 ± 71µm (mean ± s.d., n = 38 cells) apart. Thus, most (~70%) focused IEF protein peaks are minimally resolved and thus can be indexed back to a single adherent cell.

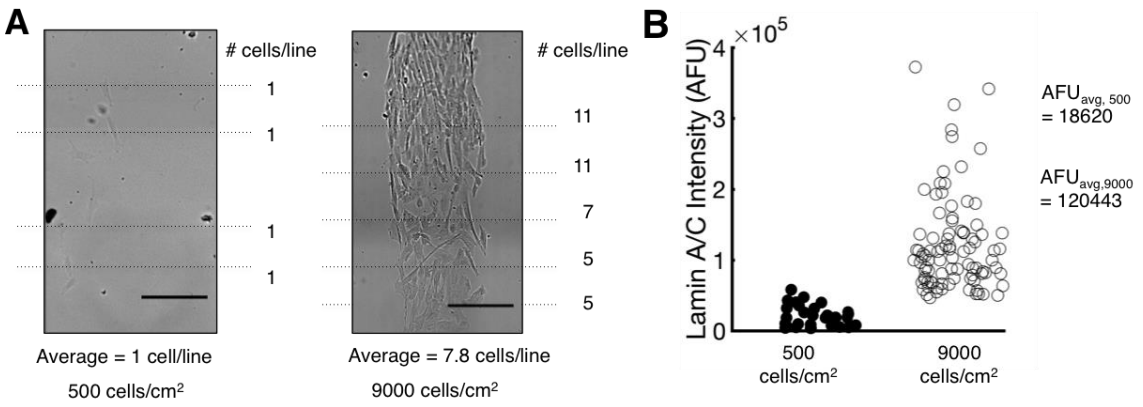

Figure S7. Analysis of total Lamin A/C content of cells indicate approximately proportional total protein content to cell density. A) Brightfield images of cells seeded at 500 and 9000 cell/cm^2 density. The total number of cells per peak were counted manually and indicated that ~7.8x the density of cells were adhered using the 9000 cell/cm^2 density, as compared to that of the 500 cell/cm^2 condition. B) Total AUC content of lamin A/C peaks that were identified. These peaks include those that were *not* minimally resolved laterally or had a Gaussian-fit threshold $R^2 <$ 0.7. In the main text, only peaks that were minimally resolved laterally with Gaussian-fit $R^2 > 0.7$ were included in the analyses. Thus, many (44%) of the peaks, which contained the highest amount of protein, were excluded.

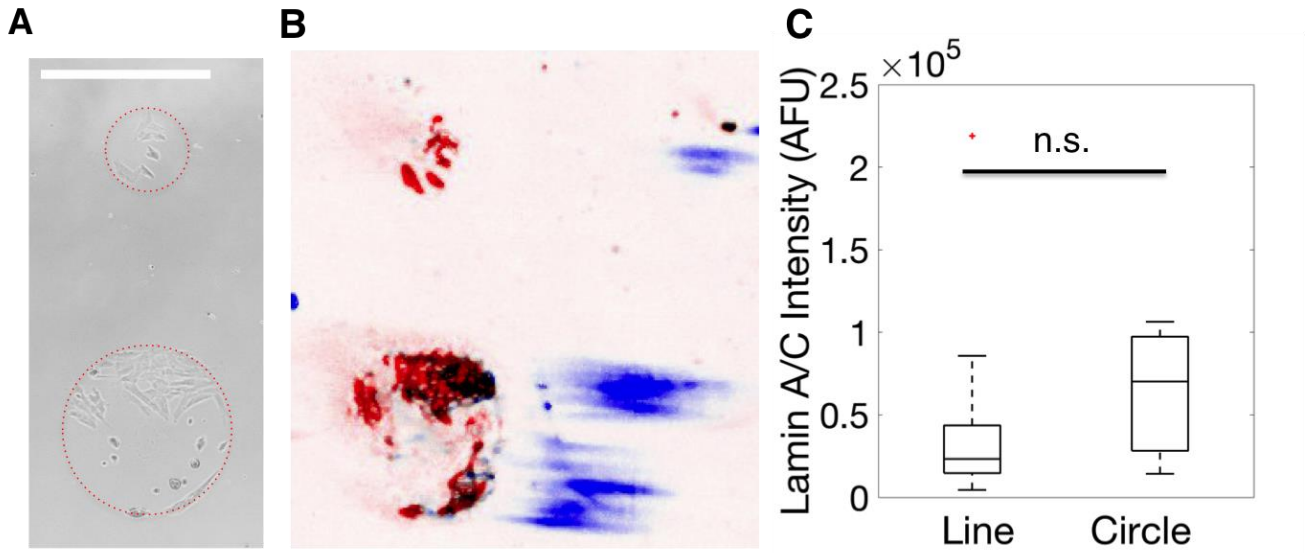

Figure S8. *In Situ* IEF of cells seeded on fibronectin-pattern islands. (A) Brightfield image of cells seeded at 9000 cells/cm^2 on islands of 200 and 500 µm diameter. (B) False-colour inverted fluorescence micrographs of lamin A/C separated via *in situ* IEF. (C) Total measured lamin A/C content between the 400-µm line and circle was not significantly different (n = 3).

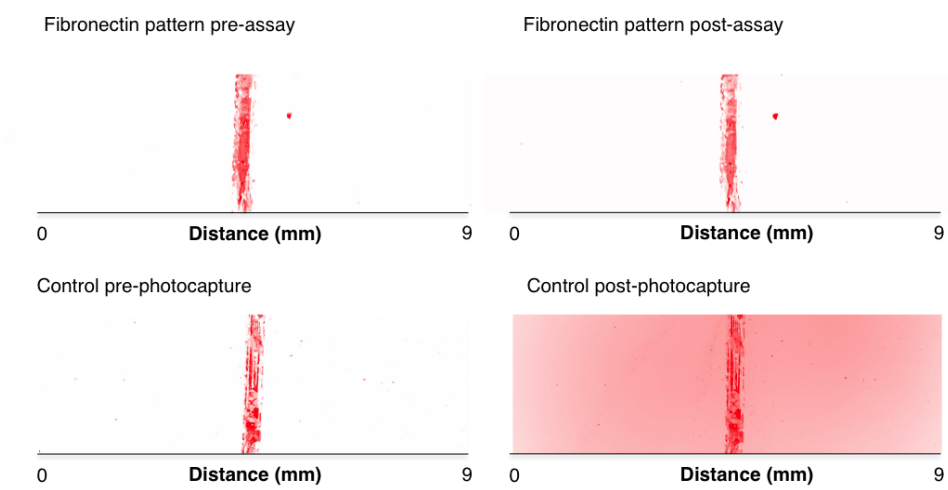

AUC (pre)	AUC (post)	% change
56609	31875	-43.7
84017	54692	-34.9
Control AUC (pre)	Control AUC (post)	
27059	35264	30.3
20692	41456	100.3

Figure S9. Comparison of fibronectin fluorescence intensity before and after *in situ* IEF. *Left*: False colored inverted fluorescence micrographs of the printed fibronectin pattern prior to seeding cells, lysis, IEF, photocapture, and immunoprobing. The fibronectin pattern did not electromigrate during the assay. *Bottom:* False colored inverted fluorescence micrographs of a printed fibronectin pattern prior to and after photocapture only. Photocapture alone increased the background intensity and the measured (background-subtracted) measured area under the curve (AUC). *Right*: Table of AUC values pre- and post-assay, and the percent change for two devices and two control devices (exposed to UV only with no other steps). Notably, the fluorescence intensity of the fibronectin pattern decreased after running the assay; however, we attribute these signal losses not to photobleaching (45 s exposure to UV for photocapture), but to other steps in the assay, such as gel sterilization, cell lysis, and multiple wash steps, as the control gel exposed only to UV actually increased in fluorescence intensity. Fibronectin is a large (~440 kDa) protein and was patterned on the substrate gel at pI~5.5, which is close to the pI of fibronectin (pI ~ 5.5-5.8). The large size and proximity to pI will limit electrophoretic mobility of the protein[4]. The increase in fluorescence intensity of the fibronectin pattern and the background signal after UV exposure is possibly attributable to benzophenone phosphorescence[5], which is currently under further examination.

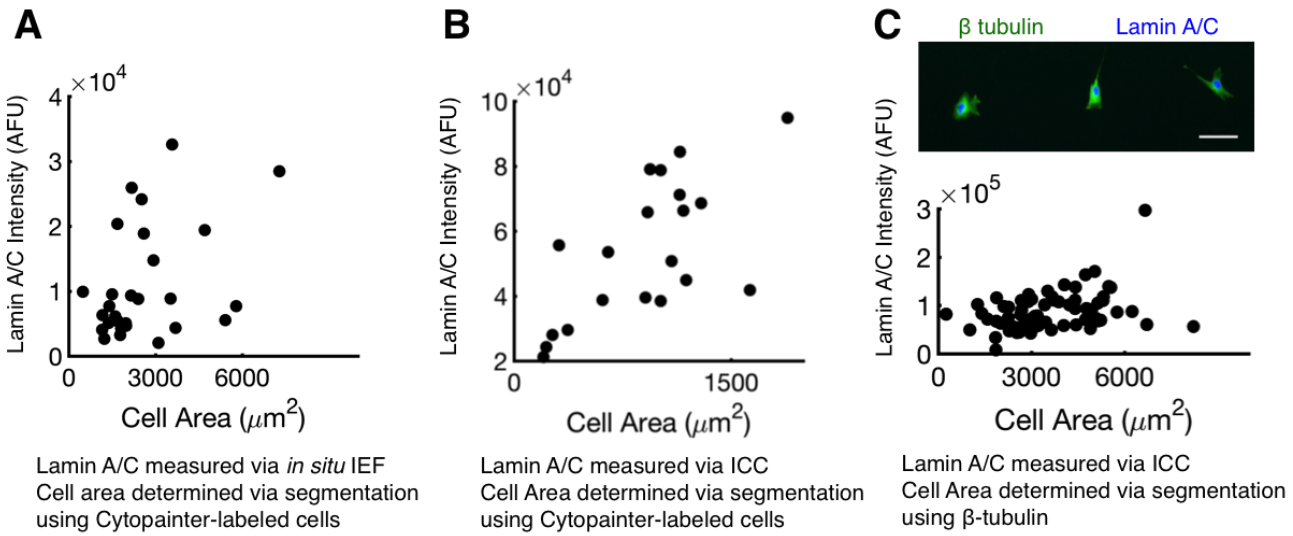

Figure S10. Lamin A/C expression does not correlate with cell morphology, as measured using a cell tracker dye (Cytopainter). (A) Scatter plot of lamin A/C intensity, as measured via *in situ* IEF (AUC + ID), which does not correlate well with cell area, as measured by segmentation using Cytopainter. (B) ICC corroborates the poor correlation of lamin A/C expression (ID) with cell area, as measured by segmentation using Cytopainter. (C) Lamin A/C intensity does correlate with area when cells are segmented using B-tubulin fluorescence. Scalebar, 100 μm. ICC, immunocytochemistry. AUC, area under the curve. ID, integrated density.

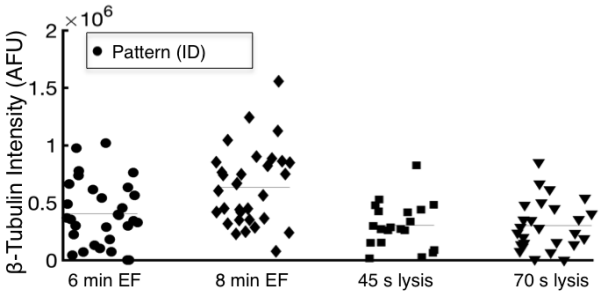

Figure S11. Comparison of ß-tubulin protein content (ID), which is retained on the fibronectin pattern, under varying lysis and EF durations. For the higher EF duration, the mean ß-tubulin protein content was higher (normal distribution from QQ plot, data not shown, and Student's two-sample t-test, $p = 0.0049$). The higher ß-tubulin content may arise from the longer assay duration, which increases duration for protein solubilisation and denaturation. Across the different lysis durations, there was no significant difference in the measured protein content (Kruskal-Wallis, $p > 0.05$) of ß-tubulin, thus suggesting that lysis times must be tuned to optimise solubilisation for different protein types. We hypothesize that transmembrane and cytoskeletal proteins, which are linked together and involved in cell anchoring, require more stringent solubilisation conditions.

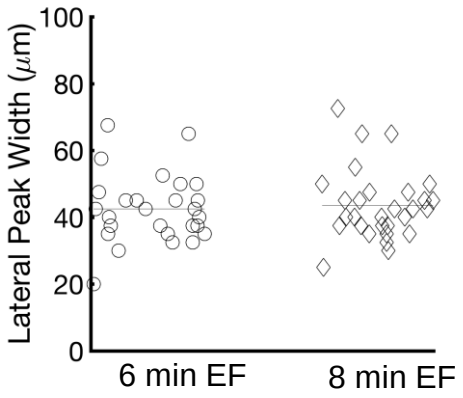

Figure S12. Scatter plot of lateral (perpendicular to IEF axis) peak width as a function of increased EF time. Lateral peak width did not change significantly. We estimated that for a 40% in gel diffusivity[3] for a 3.33%C gel and a diffusivity of lamin A/C[2] to range from 0.58-5.2, we would expect lamin A/C peak width to increase 6.1-26.7 μm from 2 additional min of electrophoresis. However, since the concentration of protein decreases exponentially away from the peak center, the lateral peak width likely did not increase measurably, as the lamin A/C falls below the limit of detection.

ESI References:

1 S. Lebel, C. Lampron, A. Royal and Y. Raymond, *The Journal of cell biology*, 1987, **105**, 1099–104.

2 V. Kochin, T. Shimi, E. Torvaldson, S. A. Adam, A. Goldman, C.-G. Pack, J. Melo-Cardenas, S. Y. Imanishi, R. D. Goldman and J. E. Eriksson, *Journal of cell science*, 2014, **127**, 2683–96.

3 J. Tong and J. L. Anderson, *Biophysical Journal*, 1996, **70**, 1505–1513.

4 P. G. Righetti, *Isoelectric Focusing: Theory, Methodology and Application: Theory, Methodology and Application*, Elsevier, 2000, vol. 2.

5 G. Wang, L. Chen and M. A. Winnik, *Macromolecules*, 1990, **23**, 1650–1653.